

3 Appendix A: Initial Data from a New High Spectral Resolution Lidar

E.W. Eloranta and P.K. Piironen

Presented at the Optical Society of America Topical Meeting
On Remote Sensing of the Atmosphere, Salt Lake City, March 1993

3.1 Introduction

The University of Wisconsin High Spectral Resolution Lidar (HSRL) has been recently redesigned for operation in an electronics semi-trailer van (ref 1). The HSRL can now be deployed in support of field experiments. This paper presents initial observations with the new configuration along with an analysis of measurement accuracy.

New measurement capabilities have been added. These include: observation of the signal variation with angular field of view, and observation of depolarization in all data channels. Depolarization measurements have been implemented by transmitting orthogonal linear polarizations on alternate laser pulses. Pulses are transmitted at $250 \mu\text{s}$ intervals such that the lidar observes the same ensemble of particles for both polarizations. Orthogonal polarizations are measured with a single detector per channel (see figure 1). Since the optical components and detector gains are identical for the two polarizations the measured depolarization ratios are independent of these factors and the system delivers very precise depolarizations. A new data channel with a computer controlled aperture allows measurements of multiple scattering as a function of receiver field of view. Since the field of view variation is dependent on the size of the scattering particles it is expected that this will allow remote measurements of cloud particle size. Other technical improvements in the new system include active control of spectrometer temperatures, greatly increased mechanical stability, an increased receiver aperture, injection of calibration signals into the signal profiles to allow continuous monitoring of system calibration drifts, and extensive computer control of system operations.

DISCLAIMER

This report was prepared as an account of work sponsored by an agency of the United States Government. Neither the United States Government nor any agency thereof, nor any of their employees, makes any warranty, express or implied, or assumes any legal liability or responsibility for the accuracy, completeness, or usefulness of any information, apparatus, product, or process disclosed, or represents that its use would not infringe privately owned rights. Reference herein to any specific commercial product, process, or service by trade name, trademark, manufacturer, or otherwise does not necessarily constitute or imply its endorsement, recommendation, or favoring by the United States Government or any agency thereof. The views and opinions of authors expressed herein do not necessarily state or reflect those of the United States Government or any agency thereof.

DISTRIBUTION OF THIS DOCUMENT IS UNLIMITED *mw*

MASTER

DISCLAIMER

**Portions of this document may be illegible
in electronic image products. Images are
produced from the best available original
document.**

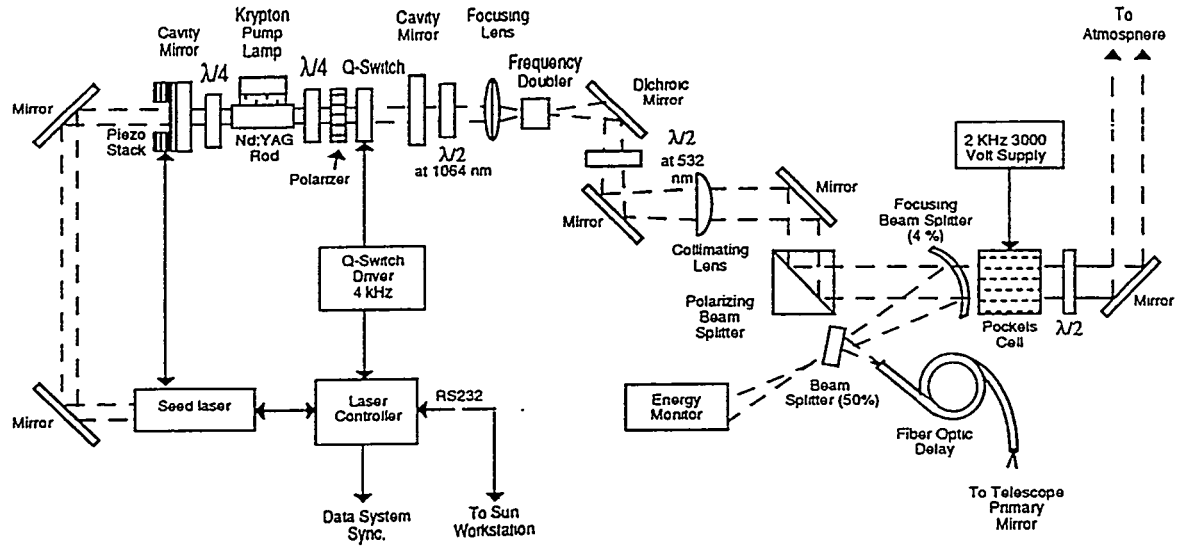


Figure 1: HSRL transmitter schematic. The transmitted polarization is rotated by 90° between successive laser pulses by a Pockels cell. A sample of each transmitted laser pulse is extracted by a beam splitter, delayed in an optical fiber and then injected into the receiver to monitor system calibration.

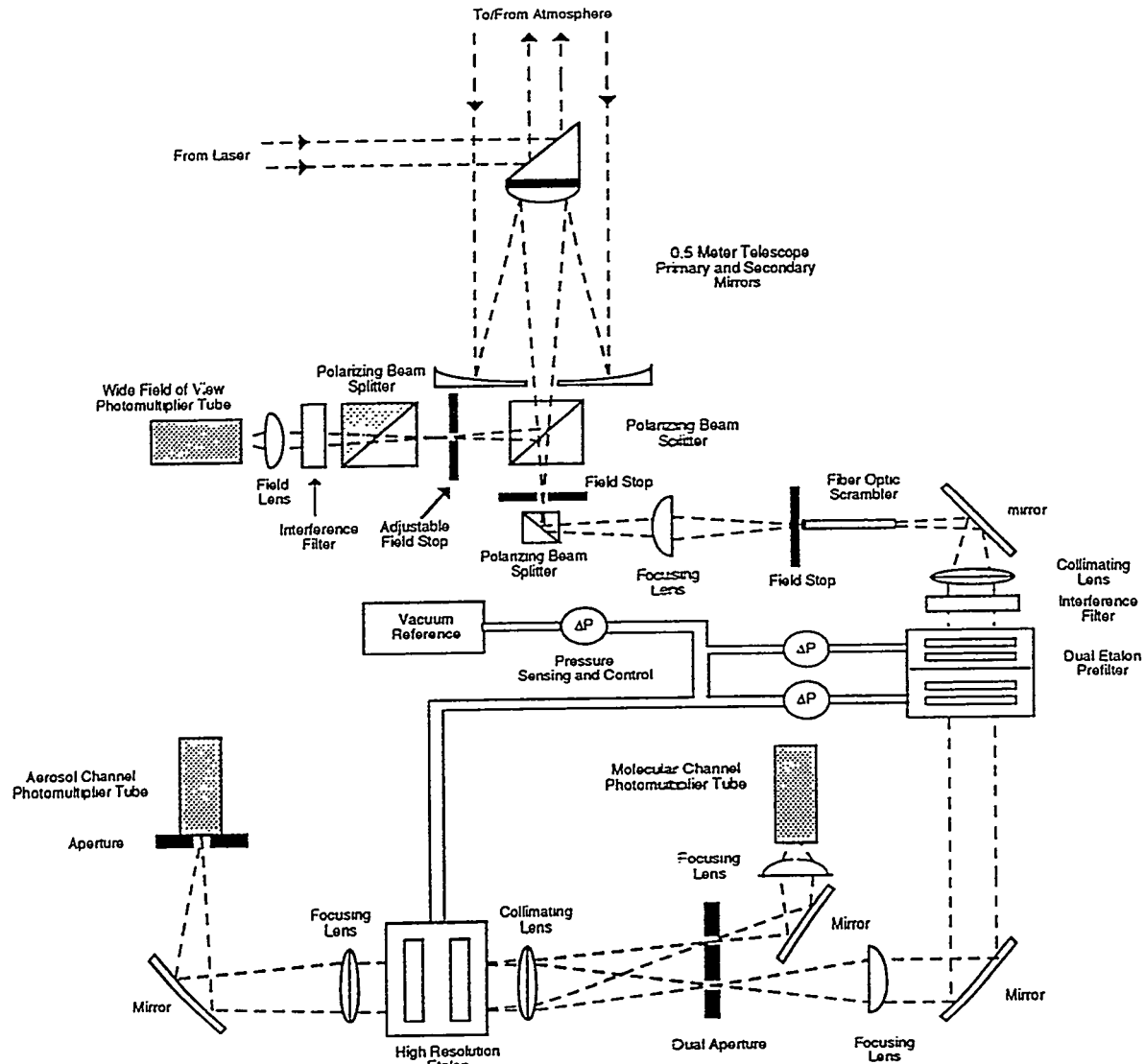


Figure 2: HSRL receiver schematic. A polarizing prism at the output of the receiving telescope separates orthogonal linear polarizations between the wide field of view channel and the spectrometer channels of the HSRL. Since the polarization of the transmitted pulse alternates between successive laser pulses each channel alternately receives parallel and perpendicular polarization components.

3.2 Backscatter cross section measurements

The HSRL divides the lidar return into separate molecular and aerosol returns. The Doppler broadening of the molecular return caused by the thermal motion is used to distinguish molecular scattering from aerosol scattering. Computing the ratio of aerosol scattering to molecular scattering and computing the molecular scattering from an independently measured density profile provides calibrated aerosol backscatter cross section measurements. These differ from estimations of backscatter cross sections made with conventional single

channel lidars. They do not require an assumed relationship between backscatter and extinction and they do not require an initial value of the scattering cross section. Furthermore the inversion is not subject to the numerical instabilities encountered in single channel lidar inversions.

Figure 3 shows separate aerosol and molecular lidar returns observed on Sept 30, 1992 along with calibrated backscatter cross sections derived for that case.

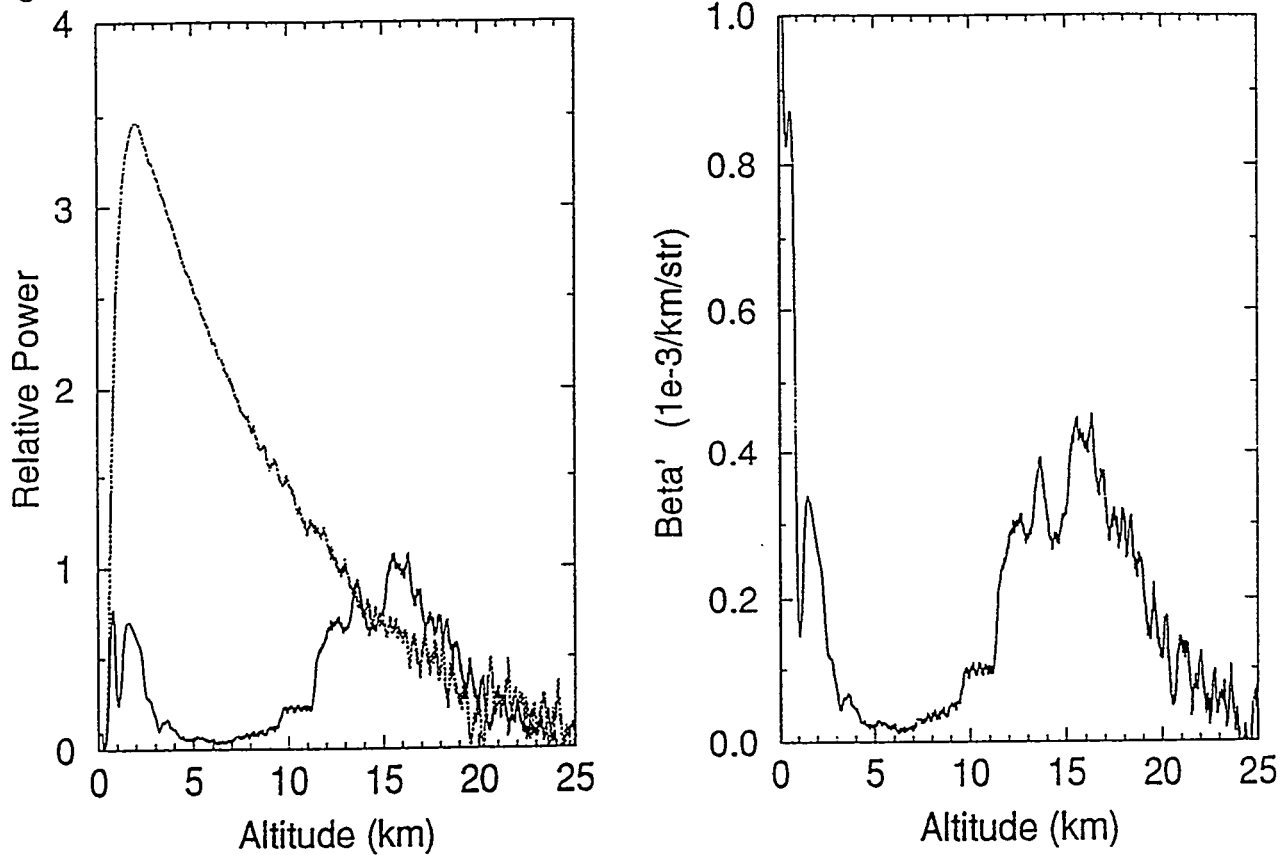


Figure 3: Separated aerosol (solid line) and molecular (dashed line) returns measured on Sept 30, 1992 are shown in the left panel. Calibrated backscatter cross sections derived from this data are shown in the right panel. Notice the strong stratospheric aerosol layer remaining from the Mt Pinatubo eruption.

3.3 Polarization measurements

Separate depolarization measurements can be made in both the "molecular" and "aerosol" channels of the HSRL while simultaneously observing the depolarization in the wide field of view channel. Calibrations show that the system contributes a depolarization of less than 0.1%. The molecular and aerosol channel signals can be inverted to separate aerosol and molecular depolarizations. This serves to demonstrate the accuracy of the HSRL depolarization measurements and to clearly show the depolarization due to aerosol particles.

Figure 5 shows inverted molecular depolarizations for the data presented in figure 4 along

with a separate case showing ice and water cloud depolarization measurements. The right panel of figure 5 shows HSRL returns from a super-cooled water cloud(at an altitude of 5 km) and from ice crystal precipitation falling from this cloud(between altitudes of 3.3 and 4.8 km). The received signals polarized parallel and perpendicular to the transmitted polarization are shown along with the depolarization ratio. Notice that the depolarization observed in the clear air below the cloud is approximately 1% and, thus very near the depolarization expected for molecular depolarization of the Cabannes line. Depolarization in the ice crystal virga is $\sim 32\%$. Also note that the water cloud depolarization is approximately 2% indicating that for this cloud the 200 microradian field-of-view of the HSRL effectively suppresses depolarization caused by multiple scattering.

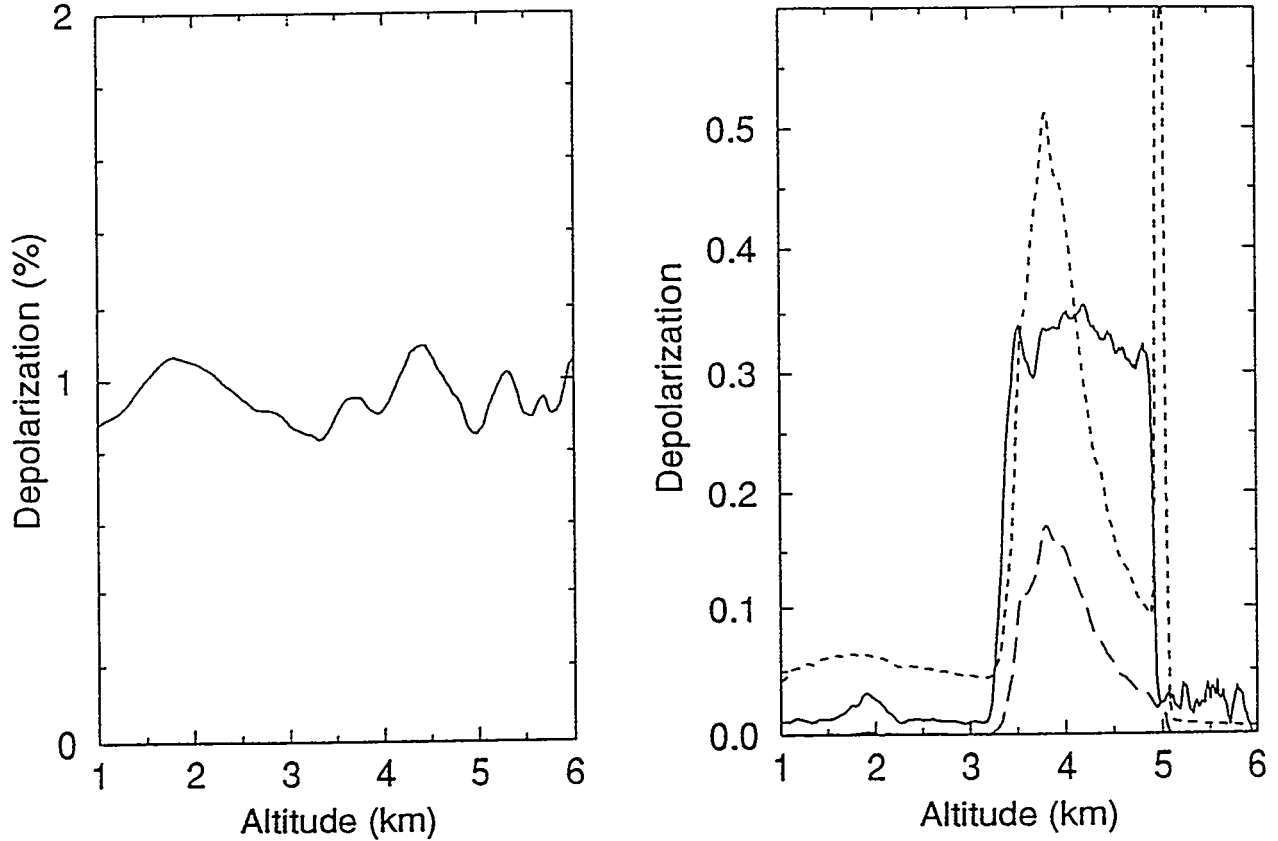


Figure 5: Depolarization measurements. The left panel shows inverted molecular depolarizations for the lidar returns presented in figure 4. Notice the small values of the depolarization; these are consistent with the depolarization expected for the Cabannes line of molecular scattering and support HSRL calibrations showing system depolarizations of less than 0.1%. The right panel shows cloud depolarizations. The uninverted molecular returns with polarization parallel and perpendicular to the transmitted polarization are shown as short dashed and long dashed lines respectively. The depolarization is shown as a solid line.